ELSEVIER

Biophysical Chemistry 109 (2004) 295–304

Biophysical Chemistry

www.elsevier.com/locate/bpc

A quantum mechanical study on phosphotyrosyl peptide binding to the SH2 domain of p56^{lck} tyrosine kinase with insights into the biochemistry of intracellular signal transduction events

Fabio Pichierri*

COE Laboratory, IMRAM, Tohoku University, 2-1-1 Katahira, Aoba-ku, Sendai 980-8577, Japan

Received 19 September 2003; received in revised form 5 December 2003; accepted 5 December 2003

Abstract

A study on the interaction between a phosphotyrosyl peptide with the SH2 domain of Lck kinase has been undertaken with the aid of semiempirical linear-scaling quantum mechanical methods. The structure of this complex has been solved at atomic resolution and, hence, it represents the ideal candidate for studying the charge deformation effects induced by the phosphopeptide on the binding site. Substantial changes in the charge of amino acid residues located in the binding pocket of the protein are observed upon ligand binding. More specifically, our quantum chemical calculations indicate that H-bonds involving charged side-chains are subject to consistent charge deformation effects whereas those forming salt bridges are unaffected by ligand binding. Furthermore, ligand binding has the effect of changing both the magnitude and direction of the protein's macrodipole, which rotates approximately 150° with respect that of the unliganded protein. This suggests that a change in the polarization state of the protein might acts as a switch during the transmission of intracellular signals. The binding energy calculated with the aid of the COSMO solvation model corresponds to about −200 kcal/mol, most of which is attributed to the interaction of the phosphotyrosine head with the amino acid chains located in the binding site of the SH2 domain.

Keywords: Phosphotyrosyl peptide; SH2 domain; Signal transduction; Quantum mechanical effects

1. Introduction

Ligand-receptor interactions that occur on the cell surface are often responsible for triggering cascades of biochemical events that conduct a variety of signals from outside to inside the cell. This phenomenon, known as signal transduction (ST), is ubiquitous for intercellular communication and regulation [1,2]. Several receptors that are found along ST pathways do possess intracellular enzymatic activity. One of these is the receptor tyrosine kinase (RTK) family [3], which catalyzes the transfer of a phosphoryl group from ATP to one of its tyrosine (Y, Tyr) residues (autophosphorylation step). The resulting phosphotyrosyl (pY, pTyr) moiety represents the epithope that interacts with the recognition domains of cognate proteins, which are integrated within the ST pathway. The subsequent phoshorylation of one of their Tyr residues (phosphorylation step), which

*Fax: +81-22-217-5110.
E-mail address: fabio@tagen.tohoku.ac.jp (F. Pichierri).

0301-4622/04/$ - see front matter © 2003 Elsevier B.V. All rights reserved.
doi:10.1016/j.bpc.2003.12.006

we have recently theoretically investigated [4], propagates downstream the signal inside the cell.

One of the most thoroughly studied recognition domains for phosphopeptides is the Src homology 2 (SH2) domain, which is composed of ~100 amino acid residues [5,6]. A search of the protein data bank (PDB) [7] reveals that, up to now, at least 80 structural determinations of the SH2 domain have been carried out either by X-ray crystallography or nuclear magnetic resonance (NMR) spectroscopy. All of the SH2 domains so far structurally characterized do contain a central antiparallel β-sheet, which is flanked by two α-helices, known as the α/β/α motif. Their co-crystallization with short phosphopeptides has led to the formulation of the so-called 'two-pronged plug two-holed socket' model [8,9]. According to this model, recognition of tyrosine phosphorylated sequences to the SH2 domain occurs through a 'rigid-body' mechanism while high-affinity binding is achieved through the insertion of pTyr in a positively charged binding pocket. In this latter regard, Waksman and co-workers [10] have recently suggested that electrostatic interactions play an important role not only for both recognition and binding but also to the specificity of the interactions that are being established at the SH2 domain-phosphopeptide interface.

Purpose of the present study is to investigate the electronic effects arising from the binding of phosphopeptide ligands to the SH2 domain by means of quantum mechanical methods. To achieve this goal, we choose to study the human $p56^{lck}$ tyrosine kinase SH2 domain in complex with a short phoshotyrosyl peptide whose structure, shown in Fig. 1, has been solved at atomic (1.0 Å) resolution by Tong et al. [11]. The protein possesses the typical α/β/α motif characteristic of the SH2 domains. High-resolution structures like this are rarely met and, hence, this complex represents the ideal candidate for a quantum mechanical (QM) study of ligand-induced charge deformation effects in proteins' active sites [12,13]. These effects have been experimentally investigated for papain [12] and acetylcholinesterase [13] by means of resonance Raman spectroscopy and fluorescence measurements, respectively. However, computational studies have been limited to investigate the effects of mutations of charged amino acid residues [14,15] whereas the effects induced by charged ligands are yet to be assessed. Besides probing the change in the residue charge for specific ligand-receptor interactions, the full QM treatment of this protein–ligand complex will be helpful in obtaining new insights into the possible implications of QM effects in the biochemistry of intracellular ST events.

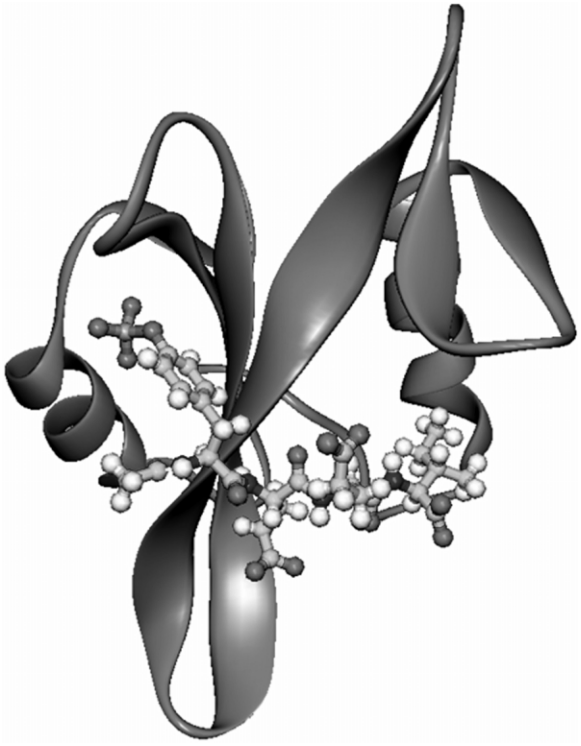

Fig. 1. Three-dimensional structure of human $p56^{lck}$ tyrosine kinase SH2 domain in complex with the phoshotyrosyl peptide (ball-and-sticks) pYEEI. The peptide ligand is wrapped around the central β-sheet with its phosphotyrosine moiety inserted between the α-helix on the left side and the nearby β-sheet.

2. Computational methods

All the calculations were performed with the MOPAC2002 software package [16]. This program is provided with Stewart's MOZYME module [17,18], which allows for the computation of very large molecular systems with performances that

Table 1
Residue sequence in the SH2 domain (PDB entry: 1LKK)

	1	2	3	4	5	6	7	8	9	10
	LEU+	GLU−	PRO	GLU−	PRO	TRP	PHE	PHE	LYS+	ASN
10	LEU	SER	ARG+	LYS+	ASP−	ALA	GLU−	ARG+	GLN	LEU
20	LEU	ALA	PRO	GLY	ASN	THR	HIS	GLY	SER	PHE
30	LEU	ILE	ARG+	GLU−	SER	GLU−	SER	THR	ALA	GLY
40	SER	PHE	SER	LEU	SER	VAL	ARG+	ASP−	PHE	ASP−
50	GLN	ASN	GLN	GLY	GLU−	VAL	VAL	LYS+	HIS	TYR
60	LYS+	ILE	ARG+	ASN	LEU	ASP−	ASN	GLY	GLY	PHE
70	TYR	ILE	SER	PRO	ARG+	ILE	THR	PHE	PRO	GLY
80	LEU	HIS	GLU−	LEU	VAL	ARG+	HIS	TYR	THR	ASN
90	ALA	SER	ASP−	GLY	LEU	CYS−	THR	ARG+	LEU	SER
100	ARG+	PRO	CYS−	GLN	THR−					

scale linearly with the number of atoms. Three semiempirical methods based on the neglect of diatomic differential overlap (NDDO) approximation [19] were employed here, namely Dewar's Austin Model 1 (AM1) [20], Stewart's Parametric Method Number 3 (PM3) [21] and the newly developed Parametric Method Number 5 (PM5) [16]. The latter method is characterized with major accuracy improvements in the heats of formation (HOF) of elements, along with a better description of hydrogen bonding (HB) interactions. All the calculations were of the single-point self-consistent field (1SCF) type, with default cutoffs of 30 Å for polarization functions and 12 Å for the NDDO approximation.

The three-dimensional structure of the human $p56^{lck}$ tyrosine kinase SH2 domain in complex with the short tetrapeptide pYEEI (pY = phosphotyrosine; E = glutamic acid; I = isoleucine) [11] was retrieved from the PDB [7] under the reference code 1LKK. The residue sequence of this protein is shown in Table 1. Since the hydrogen atoms have been included in the original atomic model, their addition was not necessary here. Hence, the protonation state of the protein, which defines the protein's net charge, corresponds to that at which the protein has been crystallized (pH 6.5) [11]. Both N,C-terminals are charged. Crystallization water molecules were removed from the experimental structure. Residues Arg134, Ser162, Tyr192, Arg207, Leu216, and Arg219 have dual side chain conformations and only conformation A has been included in the calculations (see comments inside the PDB file header).

Solvent effects were accounted for implicitly by means of the linear-scaling version [22] of the conductor-like screening model (COSMO) of Klamt and Schürmann [23]. COSMO is a continuum solvent model in which the effect of the solvent is simulated by introducing a ε-dependent correction factor into each of the NDDO hamiltonians. For water at 25 °C, we use the value of $\varepsilon = 80$.

3. Results and discussion

3.1. Charge deformation effects

As shown in Fig. 2, the bounded tetrapeptide, pYEEI, interacts with seven amino acid residues of the human $p56^{lck}$ tyrosine kinase SH2 domain. For our convenience, let us first analyze the interactions of the phosphotyrosyl moiety with the surrounding amino acid residues. The pTyr moiety, which bears two negative charges, is H-bonded to Arg134, Arg154, Ser158, and Ser164. Since the formal charge of each arginine side-chain is 1+, the binding site charge equalizes the negative charge (2−) on pTyr. Note that the H-bonds formed between each arginine side-chain with the pTyr moiety are of a different kind. Arg134 employs its NH moiety along with one terminal NH_2 group to form a pair of H-bonds with a single oxygen atom of pTyr, whereas Arg154 employs

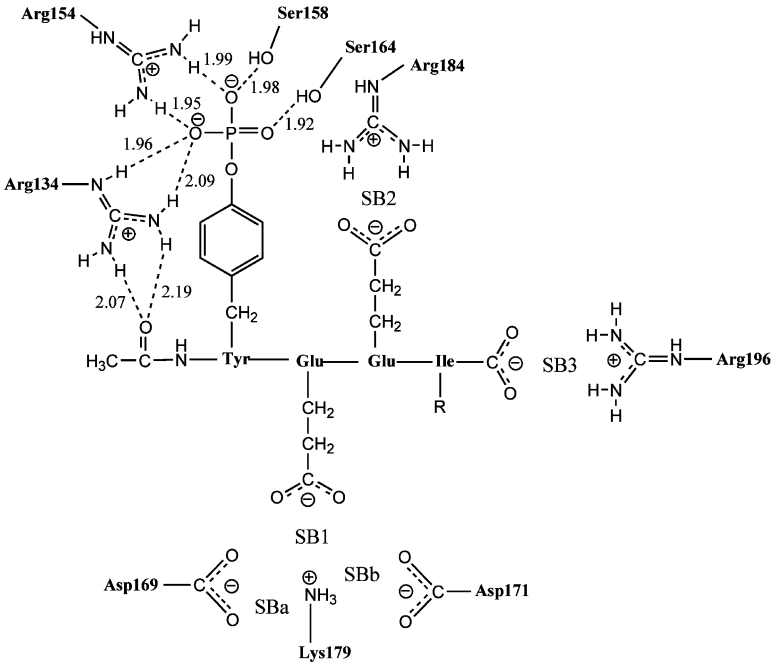

Fig. 2. Schematic view of the intermolecular interactions between the phoshotyrosyl peptide pYEEI and the side-chains of human $p56^{lck}$ tyrosine kinase SH2 domain. The five salt bridges (SB1-3 and SBa,b) are also indicated (see text). $R = C_4H_9$.

both NH_2 groups to form a pair of H-bonds with two oxygen atoms of pTyr. Since both the guanidyl and pTyr moieties are charged, these interactions can be considered as charge-assisted H-bonds. Interestingly, there exists another pair of H-bonding contacts between Arg134 and the carbonyl oxygen atom located on one terminal side of the bounded phosphopeptide. The H-bonding interactions between two oxygen atoms of pTyr and the side chains of Ser158 and Ser164 complete the binding of the phosphotyrosine head within the SH2 domain binding site pocket. The remaining non-covalent interactions of the phosphopeptide with Lys179, Arg184, and Arg196 are canonical salt-bridges [24].

Table 2 reports the side-chain charges of the five amino acid residues in the binding site of $p56^{lck}$ both in the protein–ligand (P–L) complex and in the unliganded protein, as calculated with three different NDDO methods. Since at physio-

Table 2
Side-chain Mulliken charges of selected amino acid residues in the free protein (P) and in the protein–ligand (P–L) complex as calculated with three NDDO methods and the COSMO model. The last column reports the total dipole moment (in Debye)

Method	3D	Arg134	Arg154	Ser158	Ser164	Lys179	Arg184	Arg196	Dipole
AM1 ($\varepsilon=80$)	P	1.067	1.030	0.091	0.028	1.052	1.059	1.074	136
	P–L	1.029	0.993	0.073	0.028	1.048	1.059	1.074	110
PM3 ($\varepsilon=80$)	P	1.058	1.016	0.089	0.042	1.036	1.046	1.063	137
	P–L	0.996	0.955	0.062	0.032	1.033	1.045	1.063	110
PM5 ($\varepsilon=80$)	P	1.098	1.052	0.123	0.048	1.090	1.101	1.113	136
	P–L	1.050	1.012	0.090	0.034	1.083	1.101	1.114	117

logical conditions the protein is solvated, all the above calculations were performed with the aid of the COSMO solvent model [23]. COSMO is a continuum solvent model whose linear-scaling version [22] has been shown to be very effective in studying solvated biomolecules [25]. The unliganded protein consists of 105 residues (Table 1) and its Lewis structure comprises 1763 σ bonds, 472 lone-pairs, 156 normal π bonds, 13 aromatic ring π bonds, 14 cations and 15 anions. The net charge of the unliganded system is $1-$ and, upon addition of the negatively charged $(5-)$ phosphopeptide ligand, the net charge increases to $6-$. Relaxation of the unliganded structure was not attempted since geometry optimization with MOPAC2002 is currently possible only in the gas-phase but not by employing the linear-scaling version of COSMO. We expect this limitation to be not too severe since, as found by Waksman and co-workers, only small changes have been observed between the crystal structures of the unliganded and liganded Src SH2 domain [8]. This important result led these authors to propose the so called 'rigid-body' mechanism of phosphopeptide recognition by the SH2 domain [8,9].

Let us first discuss the results obtained for the unliganded protein. As reported in Table 2, the side-chain charges of selected amino acid residues in the unliganded protein are close to the canonical charges assigned to each residue (Arg: $1+$; Lys: $1+$, Ser: 0). Differences in the net charges of identical side-chains are due to polarization effects arising from the local environment around each side-chain, along with their molecular conformation. Here, we use the term polarization to indicate an uneven distribution of electron charge density due to a polarizer, such as a charged species or group, and should be not confused with the polarization energy term arising from a decomposition analysis of the interaction energy [26,27]. The net Mulliken charges of the side-chains in the unliganded protein reported in Table 2. Apart from the differences in their conformations, we notice that Arg154, which is buried in the binding site, has lower net charge than the other three side-chains that are exposed to the solvent. At the PM5/COSMO level of theory, the difference in net charge between Arg154 and Arg196 is as large as $0.061e$. The same observation applies for both Ser158 and Ser164. The former is exposed to the solvent whereas the latter is buried into the binding site. The charge difference in this pair corresponds to $0.075e$.

When the phosphopeptide is present in the binding site of $p56^{lck}$, a change in side-chain charge is observed. In general, the magnitude of this change will depend upon the nature and topology of each specific intermolecular interaction. Let us first consider the pair of arginine residues that is H-bonded to the pTyr moiety of pYEEI. Arg154 forms a pair of charge-assisted H-bonds with two oxygen atoms of pTyr. The neighboring Arg134 residue, on the other hand, employs its NH and NH_2 moieties to H-bond a single oxygen atom of pTyr. These differences in H-bond interaction gives rise to slightly different charge effects. Upon ligand binding, the net charge of Arg134 decreases by $\sim 0.05e$ whereas that of Arg154 decreases by $\sim 0.04e$, respectively (PM5 results). Changes in net charge are also observed for both Ser158 and Ser164, both of which are H-bonded to a single oxygen atom of pTyr. The net charge of the former side-chain, however, decreases by $\sim 0.03e$ whereas the net charge of the latter decreases by $\sim 0.01e$ only, as reported in Table 2. This difference might originate from the stronger polarization to which the oxygen atom interacting with Arg134 is subject to.

The remaining three residues, namely Lys179, Arg184 and Arg196, are involved in the formation of salt bridges with pYEEI. These are pure electrostatic (i.e. Coulombic) interactions without HB contributions, as the large atom–atom distances (>5 Å) might suggest. As shown in Fig. 2, the atom–atom distances in the three salt bridges are at 5.52 Å (N•••C in SB1), 5.51 Å (C•••C in SB2), and 5.09 Å (C•••C in SB3), respectively. These distances are considerably longer than the P•••C distance of 4.20 Å in the pY/Arg154 pair where two charge-assisted H-bonds are operative. As reported in Table 2, we observe that in this case the change in net charge on going from P to P–L is practically insignificant for both Arg184 and Arg196, while the charge on Lys179 decreases by only $\sim 0.007e$ (PM5 results). It is worth noting that Lys179 forms two additional salt bridges with

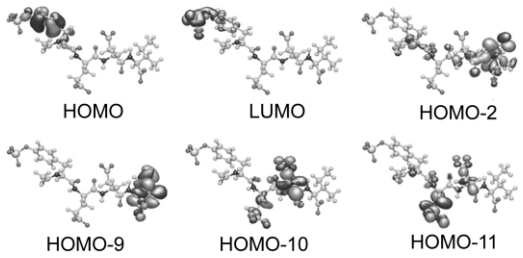

Fig. 3. Selected MO plots for pYEEI ligand in the bounded (experimental) conformation (PM5/COSMO results, $\varepsilon = 80$).

the side chains of Asp169 and Asp171 at 3.82 Å (N•••C in SBa) and 4.39 Å (N•••C in SBb), respectively. The shorter distances of SBa,b with respect to that of SB1 are indicative that the latter salt bridge is weaker than the former. Furthermore, from the three-dimensional structure of the protein we notice that Lys179 is located approximately at the centre of an isosceles triangle having the carboxyl group of Glu (E) at the vertex angle (see Fig. 2). This interesting topology of the salt bridges (SB1 and SBa,b) is likely to permit an efficient equalization of the Coulomb charge on the protein's surface.

3.2. Molecular orbital analysis

It is worth analyzing the character of the frontier MOs of the receptor and the ligand since they are expected to be responsible for the specificity of the interactions that occur at the P–L interface, as we have recently shown in a recent theoretical study of the E-Selectin/sialyl Lewis X interaction [28]. Let us start with the frontier MOs of the phosphopeptide. In Fig. 3 are shown the HOMO and LUMO levels of pYEEI, whose structure corresponds to that in the bounded (experimental) conformation. The HOMO is localized mainly on the six-membered ring of the pTyr moiety, whereas the LUMO is localized mainly on the phosphoryl group of pTyr. This feature indicates that the oxygen atoms of the pTyr head have the ability to form PO•••HN(O) H-bonds, as shown in Fig. 2. The calculated HOMO-LUMO energy gap corresponds to 8.01 eV.

It is interesting to identify the MOs that are localized on the three carboxyl groups of pYEEI that are involved in the formation of the three salt bridges (see Fig. 2). As shown in Fig. 3, the AOs of the terminal carboxyl group attached to isoleucine (I) are the highest in energy since they contribute to both HOMO-2 and HOMO-9, which are at 1.26 and 1.95 eV below the energy of the HOMO, respectively. The HOMO-10 and HOMO-11 levels, lying 2.05 and 2.1 eV below the HOMO energy, respectively, carry the contributions from the AOs of the carboxyl groups of the two glutamate (E) residues of pYEEI.

Let us now turn our attention to the FMOs of the SH2 domain. The LMOs were delocalized by employing a procedure termed canonicalization, which provides the canonical MOs. Sixteen (eight occupied and eight virtual) FMOs spanning the HOMO-LUMO energy gap were analyzed. We found that the LUMO-3 is localized on the positively charged Arg154 residue while the HOMO is found on Trp127, almost on the opposite side of the binding pocket. In the P–L complex, the HOMO is again located on Trp127; LUMO+5 is located on Arg154 while HOMO-10 is located on pTyr residue of the attached phosphopeptide and displays a character similar to that of the HOMO in the unbounded peptide (see Fig. 3). Our analysis of the frontier MOs of the SH2 domain and pYEEI indicates that only the frontier orbital interactions involving the pTyr moiety do contribute to the interaction specificity during ST while the salt bridges are likely to function as anchor points for holding in place the otherwise floppy phosphorylated tail of protein kinases.

3.3. Dipole moment

The last column of Table 2 reports the permanent dipole moment of both P and P–L as computed with three different NDDO methods, in combination with the COSMO solvation model. All the three methods yield for the unliganded $p56^{lck}$ a permanent dipole moment of approximately 136 D. This value is far smaller than those of several hundreds Debye characteristic of larger proteins. For instance, in a recent computational study on α-chymotrypsin, we computed for this protein at pH 7 a permanent dipole moment of ~492 D [29]. The large magnitude of this macro-

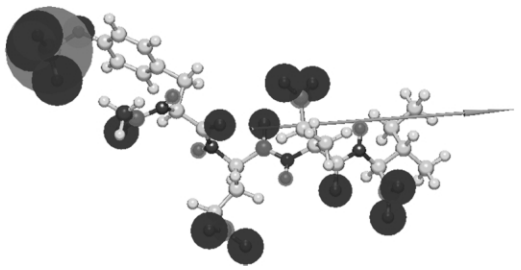

Fig. 4. Dipole moment of pYEEI (bounded conformation) and graphical representation of the Mulliken atomic charges (darker area represent negatively charged atoms) as computed with the PM5/COSMO method ($\varepsilon = 80$).

dipole has been experimentally measured with the aid of the electric dichroism technique [30]. Hence, the values reported in Table 2 reflect the fact that, apart from differences in the number of charged residues, the size of the title system (105 residues) is considerably smaller than that of α-chymotrypsin (245 residues).

Upon complexation with pYEEI, whose dipole moment corresponds to ~40 D (PM5/COSMO), as shown in Fig. 4, the permanent dipole moment of the P–L complex decreases to ~110 D. More interestingly, not only the magnitude but especially the orientation of the macrodipole changes significantly upon binding. As shown in Fig. 5, the macrodipole rotates by ~150° onto a plane perpendicular to the β-sheet motif. This indicates that a net change in the electronic charge distribution of the SH2 domain of $p56^{lck}$ tyrosine kinase might act as a switch to control the propagation of the signal inside the cell. To the best of our knowledge, this result represents the first theoretical evidence about a possible role of QM effects in ST events. For a discussion about the role of QM in biological signal processing we refer the reader to a recent paper of Matsuno and Paton [31].

3.4. Interaction energetics

It is worth estimating the binding energy of the P–L complex. Binding affinities are commonly expressed in terms of either absolute or relative binding free energies [32,33]. These can be computed at a good level of accuracy by means of molecular dynamics (MD) and/or free energy perturbation (FEP) methods, as recently shown by Helms and Wade for cytochrome p450cam [32]. The advantage in using such methods is that the computed results can be directly compared to experiments. As far as the interaction of pYEEI with the SH2 domain is concerned, isothermal titration calorimetry (ITC) yields the following thermodynamic binding parameters (at 25 °C): $\Delta G^\circ = -9.2 \pm 0.1$ kcal/mol, $\Delta H^\circ = -7.7 \pm 0.2$ kcal/mol, and $T\Delta S^\circ = 1.5 \pm 0.2$ kcal/mol [34].

Here, on the other hand, we employ QM methods to assess the absolute electronic binding energy, $\Delta E_b(s)$, of the P–L complex in continuum water environment ($\varepsilon = 80$). This means that a direct comparison with experiments is not possible. However, it is still possible to employ these energy values for comparing the relative binding affinity of different ligands towards the SH2 domain. In order to arrive at an estimate of $\Delta E_b(s)$, we employ the thermodynamic cycle shown in Fig. 6. Its use is necessary since in continuum solvent

$$E[\mathrm{P{-}L(s)}] - \{E[\mathrm{P(s)}] + E[\mathrm{L(s)}]\} \neq \Delta E_b(s) \qquad (1)$$

whereas the corresponding relation for the gas-phase is still valid. The reason for the above inequality is due to desolvation effects occurring during the formation of P–L, which cannot be

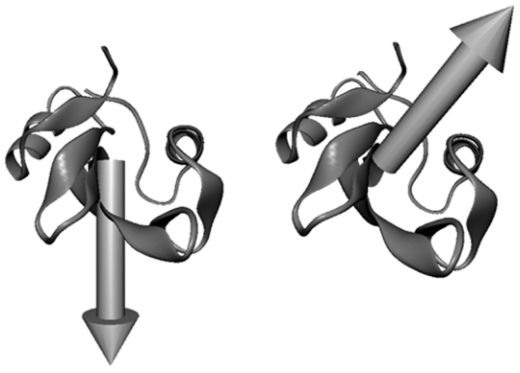

Fig. 5. Ligand-induced rotation of the SH2 domain's macrodipole (PM5/COSMO, $\varepsilon = 80$). Left: ligand-free SH2 domain; right: SH2 domain in complex with the pYEEI phosphopeptide (not shown). The protein structure has been oriented by looking down along one of the α-helices.

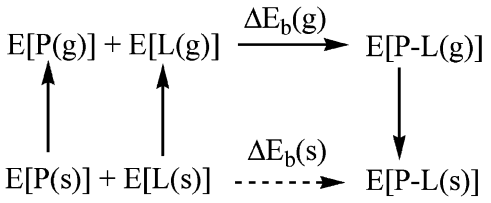

Fig. 6. Thermodynamic cycle for protein–ligand (P–L) complex formation. ΔE_b(g) and ΔE_b(s) represent the binding energies associated to the formation of the P–L complex in the gas-phase (g) and water (s), respectively.

accounted for with our continuum (i.e. implicit) solvation approach. In other words, the contribution arising from the solvent molecules located near the binding pocket that are being replaced by L upon binding to P cannot be evaluated with a continuum solvent model such as COSMO. Hence, a thermodynamic cycle like that shown in Fig. 6 must be employed. Starting from P(s) and L(s), we can imagine to desolvate them so as to arrive at the corresponding specie in the gas-phase, namely P(g) and L(g). Upon formation of P–L(g), the complex is solvated to yield P–L(s).

The heats of formation corresponding to E[P–L(g,s)], E[P(g,s), and E[L(g,s)], as computed both in continuum water ($\varepsilon=80$) and in the gas-phase and by employing three different semiempirical NDDO methods, are reported in Table 3. The binding energies computed with these three methods are in excellent agreement with each other, being −200 kcal/mol at the AM1 level, −214 kcal/mol at the PM3 level and −210 kcal/mol at the PM5 level. Note that the corresponding binding energy values calculated in the gas-phase are approximately 100 kcal/mol larger (i.e. more negative) than those values computed with the procedure described above. In contrast, when ΔE_b(s) is calculated simply by subtracting E[P(s)] and E[L(s)] from E[P–L(s)] the resulting energy value is positive.

Finally, it is interesting to assess how each intermolecular interaction contributes to the total binding energy. Since we are aware that semiempirical methods are not best suited to accurately compute the binding energies of interacting fragments [27], we decided to estimate the interaction energy (in kcal/mol) associated to each salt bridge by means of the following (empirical) equation

$$E_{SB}=(332/\varepsilon)*(q_1q_2/r_{12}) \quad (2)$$

where ε is the dielectric constant of the medium and q_i ($i=1,2$) the ion-pair charges separated by r_{12} [35]. Excluding pY, the PM5 charges calculated for the charged groups of pYEEI are: $-0.905e$ for the side chain of Glu (E) in SB1, $-0.894e$ for the side chain of Glu (E) in SB2, and $-0.668e$ for the terminal carboxyl group attached to Ile (I) in SB3 (see Fig. 2). The choice of ε is critical. Using the value $\varepsilon=10$, which has been assigned by Warshel and co-workers [36] to the active site regions of proteins, we estimate interaction energies of −5.9 kcal/mol for both Lys179/Glu (SB1, $r_{12}=5.52$ Å) and Arg184/Glu (SB2, $r_{12}=5.51$ Å) salt bridges, and −4.8 kcal/mol for the Arg196/Ile (SB3, $r_{12}=5.09$ Å) salt bridge. These estimates are in excellent agreement with those of approxi-

Table 3
Heats of formation (HOF, kcal/mol) of the protein-ligand complex and its separated components as calculated with three different NDDO methods in the gas-phase and in continuum water ($\varepsilon=80$). The last column reports the binding energy (ΔE_b(s), kcal/mol) as computed from the thermodynamic cycle of Fig. 6

Method	HOF			ΔE_b(s)
	Protein–Ligand	Protein	Ligand	
AM1	2103.45873	2499.571778	−75.740584	
AM1 ($\varepsilon=80$)	−401.951567	434.649307	−956.913738	**−200**
PM3	893.624797	1334.098495	−112.560609	
PM3 ($\varepsilon=80$)	−1719.910210	−845.983899	−987.535956	**−214**
PM5	−616.519564	17.137718	−300.904954	
PM5 ($\varepsilon=80$)	−3544.251357	−2454.104776	−1212.750633	**−210**

mately −5 kcal/mol obtained with simpler models [35]. Hence, we can conclude that the three salt bridges formed at the SH2-phosphopeptide interface contribute to only a small fraction (approx. 2%) of the total binding energy. It follows that binding is achieved through the eight H-bonds, six of which do involve the pTyr head, as shown in Fig. 2.

4. Conclusions

We have investigated the charge effects induced by the binding of a phosphotyrosyl peptide to the human $p56^{lck}$ tyrosine kinase SH2 domain. Our analysis indicates that change in net charge of amino acid side-chains depend upon both the nature and topology of the observed interactions. For instance, charge-assisted H-bonds are responsible for stronger charge deformation effects in comparison to H-bonds where charge-assistance does not occur. Salt bridges, on the other hand, do not affect the net charge of protein side-chains upon ligand binding and, hence, their contribute little to the binding energy. From the present QM treatment we have also calculated the macrodipoles of both P and P−L and observed a relatively small (approx. 20 Debye) change in magnitude but a substantial change in their orientations. This result indicates the possibility that, upon binding, the phosphopeptide can induce a change in the electronic polarization of the SH2 domain thereby acting as a switch with respect to the transmission of intracellular signals. This interesting computational result represents a possible signature of QM effects in the biology of signal transduction.

Acknowledgments

The author is thankful to Fujitsu Ltd. (Tokyo) for providing the MOPAC2002 software package. Financial support for this work has been provided by the 21st century Center of Excellence (COE) program ‘Giant Molecules and Complex Systems’ of MEXT hosted at Tohoku University.

References

[1] K.M. Eyster, Introduction to signal transduction. A primer for untangling the web of intracellular messengers, Biochem. Pharmacol. 55 (1998) 1921–1938.

[2] G. Krauss, Biochemistry of Signal Transduction and Regulations, Wiley-VCH, Weinheim, 2001.

[3] S.R. Hubbard, J.H. Till, Protein tyrosine kinase structure and function, Annu. Rev. Biochem. 69 (2000) 373–398.

[4] F. Pichierri, Y. Matsuo, Mechanism of tyrosine phosphorylation catalyzed by the insulin receptor tyrosine kinase: a semiempirical PM3 study, J. Mol. Struct. (Theochem) 622 (2003) 257–267.

[5] I. Sadowski, J.C. Stone, T. Pawson, A non-catalytic domain conserved among cytoplasmic protein-tyrosine kinases modifies the kinase function and transforming activity of Fujinami sarcoma virus P130gag-fps, Mol. Cell. Biol. 6 (1986) 4396–4408.

[6] M.F. Moran, C.A. Koch, D. Anderson, C. Ellis, L. England, G.S. Martin, et al., Src homology region 2 domains direct protein-protein interactions in signal transduction, Proc. Natl. Acad. Sci. USA 87 (1990) 8622–8626.

[7] H.M. Berman, J. Westbrook, Z. Feng, G. Gilliland, T.N. Bhat, H. Weissig, et al., The Protein Data Bank, Nucleic Acids Res. 28 (2000) 235–242.

[8] G. Waksman, S.E. Shoelson, N. Pant, D. Cowburn, J. Kuriyan, Binding of a high affinity phosphotyrosyl peptide to the Src SH2 domain: crystal structures of the complexed and peptide-free forms, Cell 72 (1993) 779–790.

[9] J.M. Bradshow, R.A. Grucza, J.E. Ladbury, G. Waksman, Probing the ‘two-pronged plug two-holed socket’ model for the mechanism of binding of the Src SH2 domain to phosphotyrosyl peptides: a thermodynamic study, Biochemistry 37 (1998) 9083–9090.

[10] R.A. Grucza, J.M. Bradshaw, V. Mitaxov, G. Waksman, Role of electrostatic interactions in SH2 domain recognition: salt-dependence of tyrosyl-phosphorylated peptide binding to the tandem SH2 domain of the Syk kinase and the single SH2 domain of the Src kinase, Biochemistry 39 (2000) 10 072–10 081.

[11] L. Tong, T.C. Warren, J. King, R. Betageri, J. Rose, S. Jakes, Crystal structures of the human $p56^{lck}$ SH2 domain in complex with two short phosphotyrosyl peptides at 1.0 A and 1.8 A resolution, J. Mol. Biol. 256 (1996) 601–610.

[12] P.R. Carey, R.G. Carriere, D.J. Phelps, H. Schneider, Charge effects in the active site of papain: resonance Raman and absorption evidence for electron polarization occurring in the acyl group of some acylpapains, Biochemistry 17 (1978) 1081–1087.

[13] H.-J. Nolte, T.L. Rosenberry, E. Neumann, Effective charge on acetylcholinesterase active sites determined from the ionic strength dependence of association rate constants with cationic ligands, Biochemistry 19 (1980) 3705–3711.

[14] T. Simonson, G. Archontis, M. Karplus, A Poisson-Boltzmann study of charge insertion in an enzyme active site: the effect of dielectric relaxation, J. Phys. Chem. B 103 (1999) 6142–6156.

[15] V. Dillet, R.L. Van Etten, D. Bashford, Stabilization of charges and protonation states in the active site of the protein tyrosine phosphatases: a computational study, J. Phys. Chem. B 104 (2000) 11 321–11 333.
[16] J.J.P. Stewart, MOPAC2002 (version 1.0), Fujitsu Ltd. (Tokyo).
[17] J.J.P. Stewart, Application of localized molecular orbitals to the solution of semiempirical self-consistent field equations, Int. J. Quantum Chem. 58 (1996) 133–146.
[18] J.J.P. Stewart, in: Encyclopedia of Computational Chemistry, John Wiley and Sons, 1998.
[19] W. Thiel, Perspectives on semiempirical molecular orbital theory, Adv. Chem. Phys. 93 (1996) 703–757.
[20] M.J.S. Dewar, E.G. Zoebish, E.F. Healy, J.J.P. Stewart, Development and use of quantum mechanical molecular models. 76 AM1: a new general purpose quantum mechanical molecular model, J. Am. Chem. Soc. 107 (1985) 3902–3909.
[21] J.J.P. Stewart, J. Comput. Chem. 10 (1989) 209–220.
[22] D.M. York, T.-S. Lee, W. Yang, Parameterization and efficient implementation of a solvent model for linear-scaling semiempirical quantum mechanical calculations of biological macromolecules, Chem. Phys. Lett. 263 (1996) 297–304.
[23] A. Klamt, G. Schüürmann, COSMO: a new approach to dielectric screening in solvents with explicit expressions for the screening energy and its gradient, J. Chem. Soc. Perkin Trans. 2 (1993) 799–805.
[24] S. Kumar, R. Nussinov, Salt bridge stability in monomeric proteins, J. Mol. Biol. 293 (1999) 1241–1255.
[25] J. Khandogin, A. Hu, D.M. York, Electronic structure properties of solvated biomolecules: a quantum approach for macromolecular characterization, J. Comput. Chem. 21 (2000) 1562–1571.
[26] A. van der Vaart, K.M. Merz Jr, The role of polarization and charge transfer in the solvation of biomolecules, J. Am. Chem. Soc. 121 (1999) 9182–9190.
[27] P.L. Cummins, S.J. Titmuss, D. Jayatilaka, A.A. Bliznyuk, A.P. Rendell, J.E. Gready, Comparison of semiempirical and ab initio QM decomposition analyses for the interaction energy between molecules, Chem. Phys. Lett. 352 (2002) 245–251.
[28] F. Pichierri, Y. Matsuo, Effect of protonation of the *N*-acetyl neuraminic acid residue of sialyl Lewis X: a molecular orbital study with insights into its binding properties toward the carbohydrate recognition domain of E-selectin, Bioorg. Med. Chem. 10 (2002) 2751–2757.
[29] F. Pichierri, Computation of the permanent dipole moment of α-chymotrypsin from semiempirical linear-scaling quantum mechanical methods, J. Mol. Struct. (Theochem) 664–665 (2003) 197–205.
[30] J. Antosiewicz, D. Porschke, The nature of protein dipole moments: experimental and calculated permanent dipole of α-chymotrypsin, Biochemistry 28 (1989) 10 072–10 078.
[31] K. Matsuno, R.C. Paton, Quantum mechanics in the present progressive mode and its significance in biological information processing, Biosystems 49 (1999) 229–237.
[32] V. Helms, R.C. Wade, Computational alchemy to calculate absolute protein-ligand binding free energy, J. Am. Chem. Soc. 120 (1998) 2710–2713.
[33] S. Boresch, F. Tettinger, M. Leitgeb, M. Karplus, Absolute binding free energies: a quantitative approach to their calculation, J. Phys. Chem. B 107 (2003) 9535–9551.
[34] J.M. Bradshow, G. Waksman, Calorimetric examination of high-affinity Src SH2 domain-tyrosyl phoshopeptide binding: dissection of the phosphopeptide sequence specificity and coupling energetics, Biochemistry 38 (1999) 5147–5154.
[35] G.E. Shulz, R.H. Schirmer, Principles of Protein Structure, Springer, New York, 1979.
[36] A. Warshel, A. Papazyan, Electrostatic effects in macromolecules: fundamental concepts and practical modeling, Curr. Op. Struct. Biol. 8 (1998) 211–217.